Reliable Handover Prediction and Resource Allocation in MEO Mobile Satellite networks

Iordanis Koutsopoulos and Leandros Tassiulas
Department of Electrical Engineering and Institute for Systems Research
University of Maryland at College Park, College Park, MD 20742, USA
{jordan, leandros}@isr.umd.edu

Abstract— **Efficient satellite resource management and allocation techniques aim at providing reliable real-time service, taking into consideration the scarcity of resources and the large number of handovers. We present an algorithm for reliable satellite and beam handover prediction at the SBS, based on a combined UT position and received signal strength criterion. UT position determination is achieved by introducing a new satellite-based coordinate system and received signal strength is calculated by using a simplistic channel propagation model. The probability of a handover event is calculated analytically and the performance of the algorithm is analyzed in terms of UT mobility or stationarity. An alternative criterion for beam handover is proposed, where path selection depends on maximum residence time in a beam. Results show a significant reduction of beam handover rate and consequently of signalling overhead after adopting this criterion.**

Keywords— **Mobile satellite networks, handover prediction, UT mobility, channel propagation model**

I. Introduction

In order to extend the availability of communications services and finally provide global coverage, several satellite systems have been proposed as a supplement to already existing terrestrial networks. To provide service for small mobile or hand-held terminals, MEO and LEO non-geostationary systems are an appealing solution. The traffic generated by a User Terminal (UT), is supported by satellites successively passing over the service zone, and must be handed over from one satellite to the next. Moreover, diversity attribute is provided as a means of mitigating unpredictable call blockage [2].

Several scenarios for efficient handover and resource allocation have prevailed in literature. In the context of satellite handover, two strategies have been proposed [3]: Maximizing the instantaneous elevation angle or minimizing the handover rate for a user. In the former case, that satellite providing the highest elevation angle is selected, whereas in the latter case a satellite is chosen for as long as it remains visible.

The standard procedure of beam signal level monitoring, applied in cell reselection schemes in GSM terrestrial cellular networks is analyzed in [4] in the context of a satellite system. The proposed scheme may be integrated or optimized with a positioning system (e.g GPS), but it can also work without that.

One of the major problems in wireless networks is the large amount of exchanged signalling information. Due to reduction of the beams' size in non-GEO satellite systems, the number of handovers tends to increase. In order to save valuable satellite resources, signalling information must be kept to a minimum. In that aspect, *seamless handover* is a smart approach for TDMA-based systems, since it does not interrupt the call and requires minimum signalling exchanges [5].

We investigate Handover prediction and resource allocation techniques. In section II we build the basic setup and mention preliminaries of a mobile satellite system and in section III the proposed Path Selection algorithm is analyzed. Section IV provides an insight into satellite and beam handover, examines the impact of UT mobility and turns attention in the maximum beam residence criterion, and section V presents our propagation model. Finally in section VI numerical results are illustrated and conclusions follow.

II. Preliminary structures and principles

The satellite component of a mobile satellite system essentially consists of r SBSs, n satellites with m beams per satellite footprint and a traffic distribution assignment according to a population of mobiles.

A. Geographical coordinate systems

To record the position of a satellite, SBS or UT, the following coordinate systems are considered:
1. ECI (Earth Centered Inertial) System : This system is based at the earth center. The x-axis is fixed towards vernal equinox and the z-axis is the polar axis.
2. ECEF (Earth Centered Earth Fixed) system : This system is based at the earth center and rotates with it. The positive x-axis points towards the intersection of the prime meridian and the equator (0^o longitude and latitude) and the z-axis is the polar axis [1].
3. OF (Orbit Frame): Our innovation comprises this satellite-based system. Its x-axis points in the direction of the satellite, the positive z-axis points towards earth center and y-axis completes a right-handed triplet. This system provides a simple pictorial representation of the beam pattern, overcoming complicated patterns on the curved earth surface and is used in beam handover prediction. A point on the earth surface is mapped onto a two dimensional system (the z-dimension gets eliminated), so that residence within a satellite footprint s_i and a specific beam b_j can be easily detected. The transformation method from the ECEF to the OF system is provided in Appendix A.

B. Beam pattern

By introducing the azimuth ϕ_i, elevation θ_i and half power beam width β_i angles in the OF coordinate system, each

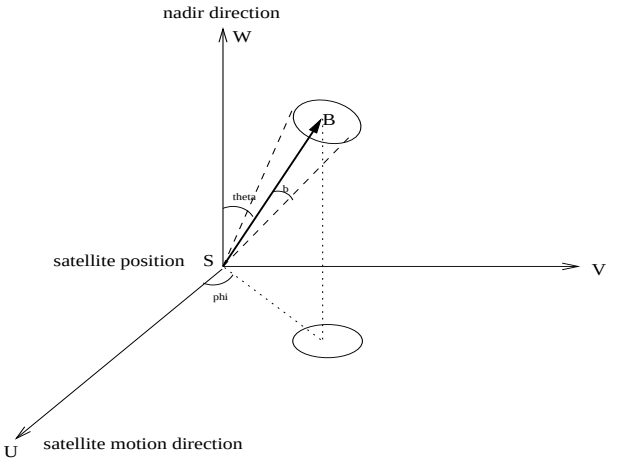

Fig. 1. Illustration of a beam position in the OF coordinate system.

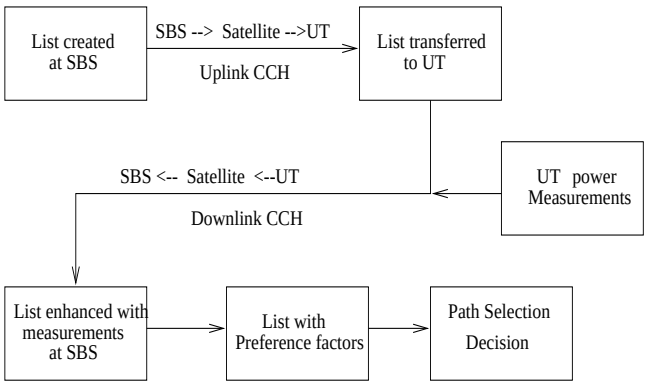

Fig. 2. Schematic representation of Path Selection procedure.

beam b_i is uniquely defined in the OF plane by a position vector of the beam center relative to the satellite nadir:

$$\vec{W}_i = sin\theta_i cos\left(\phi_i + \frac{3\pi}{2}\right)\hat{x} + sin\theta_i sin\left(\phi_i + \frac{3\pi}{2}\right)\hat{y} \quad (1)$$

and its radius $R_i = tan\,(\beta_i/2)$.

III. Basic algorithms executed at the SBS

A. Algorithm A: Beam selection for power measurements

In order to ensure the most appropriate cell selection at a transition, each UT continuously monitors the received BCCH signal of a proper set of adjacent satellite cells. The SBS periodically commands the UT to measure the BCCH signal strength of all visible serving and non-serving satellites and creates a list of the beams that will provide measurements and will serve as a confirmation to handover decisions. The list comprises a set $\mathcal{C}$ of beams currently covering the UT position and belonging to visible satellites from both the UT and the SBS, and a set $\mathcal{A}$ of approaching beams of serving satellites. The above sets of beams are candidates for a satellite and a beam handover respectively. Upon reception of this list via an uplink Common Control Channel (CCH), the UT performs measurements for each of these beams and sends the enhanced list back to the SBS on the downlink CCH. This procedure takes place both during signalling and traffic phase of a call and is depicted in firure 2.

B. Algorithm B: Path Selection

Path Selection algorithm provides the input to Resource Allocation and takes place after Algorithm A and before a handover of any type or a non-diversity to diversity transition attempt. Each entry e_i of the list is initially a pair of satellite and beam indices (s_i, b_i). The list is modified as follows:
1. All possible combinations (e_i, e_j) of single elements are created and appended to the list.
2. Entries with a power measurement below a given threshold are eliminated, as indicating unreliable connection.
3. Double entries including an overloaded satellite are eliminated, as not eligible for diversity.
4. The list is ranked according to a predefined preference factor. Finally the first node of the list will have the highest preference factor.
Each entry of the list represents a single or a diversity path, eligible for resource allocation. For each entry k the associated Preference Factor P_k is a function of the satellite elevation angle θ_k, the signal level I_k and the azimuth separation angle ϕ_k, in case the node denotes a diversity path. Thus

$$P_k = A \times \left(\frac{\theta_{k,1}}{\pi} + \frac{\theta_{k,2}}{\pi} + \frac{\phi_{k,12}}{2\pi}\right) + B \times (I_{k,1} + I_{k,2}) \quad (2)$$

In the above equation I_k is a variable illustrating the difference of the received signal level from the threshold value. The received signal strength is computed with a simplistic channel propagation model that takes into consideration UT position in a beam, multipath fading loss, shadowing loss and free space loss. A big azimuth angle provides a preferable path, since there are fewer chances that both paths will be corrupted due to an unpredictable blockage.

IV. Criteria for satellite and beam handover

A. Beam Handover

UT position is mapped to OF through a matrix, whose elements depend on current satellite position and velocity. This ephemeris data is used to determine future satellite locations, so that future positions of the UT in the OF are known. A binary search method of successive mappings of UT position to the OF determines the time to handover to virtually any desired accuracy (other errors notwithstanding).

When a UT enters a beam, it is mapped to the OF several times until a time interval of acceptable length (e.g. 1 minute) is found, where the UT resides in the current beam at the beginning of the interval and lies in a different beam at the end of the interval (Figure 3). Handover must occur sometime during this interval and predicted handover time is the midpoint of the interval. If the acceptable time inaccuracy is 1 minute, the handover prediction algorithm is accurate within 30 seconds. Equivalently, the contribution to the error in handover prediction is at most 30 seconds in this case. In reality several other factors contribute to prediction error, such as ephemeris data and UT position inaccuracy and UT mobility.

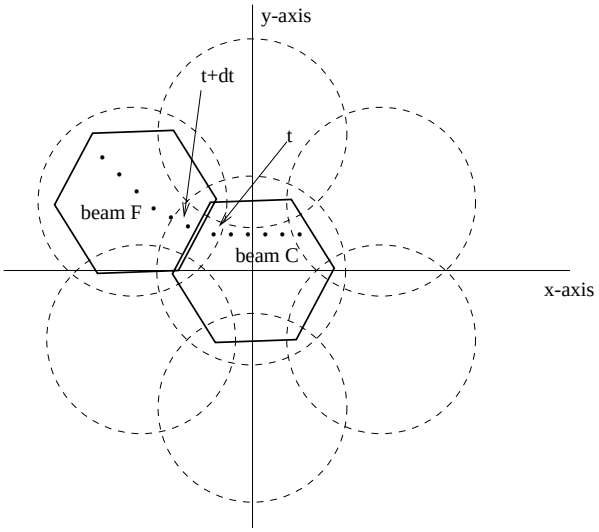

Fig. 3. Demonstration of beam handover from the beam located in the satellite nadir to a neighboring beam.

Assuming an initial horizon window length of W_0 minutes and an acceptable time prediction error of δ seconds, the number of OF mappings before convergence is at most:

$$N = \left\lceil \log_2 \frac{60W_0}{\delta} \right\rceil \tag{3}$$

B. Mobility impact in Beam Handover time

We presented an efficient algorithm for Beam Handover prediction under the assumption of a stationary UT. It is conceivable that successive handover predictions for an extended call may degrade to an unacceptable point, when the UT is in motion. The purpose of this subsection is to study the effects of UT mobility and propose a solution.

We assume that a UT experiences a beam transition when the received signal level from two adjacent beams, the current and the upcoming, are equal. A handover will nominally occur at a beam transition. However, factors such as measurement and position error, fading etc. will affect handover time.

The spot beams move at different rates relative to the earth surface, as they follow different paths around the earth. Edge beams conceptually move at lower rates than central ones. UT velocity will have the greatest effect on beam transitions in the slowest moving beams and the least effect in the fastest moving ones. Let the functions $V_c(t)$ and $V_e(t)$ denote the velocity magnitudes of beams located in the center and in the edge of a satellite footprint respectively and let $V_{c,min}$, $V_{e,min}$ be their minimum values. Then, in the worst case where the UT and the beam move in opposite directions, an impact of at most $q = V_{ut}/V_{c,min}\%$ and $p = V_{ut}/V_{e,min}\%$ should be anticipated for UT moving in a central or an edge beam and therefore the actual transition time will decrease by this amount. Consider the case when a mobile experiences n successive handovers at times t_i, $1 \leq i \leq N$ and moves along edge beams. If the mobile is stationary, it will experience the n-th transition at time $t_{stat,n} = \sum_{i=1}^{n} t_i$ whereas if it moves in the opposite direction of that of the beam the time is

$$t_{mob,n} = \sum_{i=1}^{N} t_i (1-p)^{N-i+1} \tag{4}$$

C. Satellite Handover

For the satellite handover we have the procedure:

- Obtain the serving satellite(s) at current time t_c.
- Update those to a future time t_f, using the satellite ephemeris data.
- If $\theta_{UT}(t_f) \leq 10^o$ or $\theta_{SAN}(t_f) \leq 10^o$, then conclude that a satellite handover has occurred at some time $t^* \epsilon\, (t_c, t_f)$.
- Apply bisection idea on that interval.
- Stop after n^* iterations when $t_{f,n^*} - t_{c,n^*} < W$.
- The predicted satellite handover time is thus

$$t_s = \frac{t_{f,n^*} + t_{c,n^*}}{2} \tag{5}$$

D. Maximum beam duration criterion for beam handover

Motivated by the fact that additional handover occurances contribute to excess signalling load and significant transmission delays in the system, we propose a new criterion for handover event triggering. The basic characteristic is the minimization of satellite and beam handover rates, since the residence time in a cell is forced to be the maximum possible. Upon creation of the list with the candidate paths for transition, no preference factor computation is required. Simply the node containing the beam in which the mobile is predicted to stay the longest is selected as the transition beam. This beam may belong to the current serving satellite or not, providing thus the definition of beam handover or satellite handover after adopting this criterion.

This criterion is computationally less intensive than Path Selection. UT residence time for each beam in the list is computed by standard mappings in the OF satellite coordinate system and no elevation angle computation is required. More importantly, no power measurement information exchange between the UT and the SBS is necessary in order to confirm handover decisions.

V. Channel Propagation model

A simplistic channel propagation infrastructure is required in order to model the received signal strength which supports handover decisions. The received signal is a function of the free space loss, the UT position in a beam, the multipath fading loss and the shadowing loss.

A. Free Space Loss

The signal experiences a free space loss which is proportional to the distance r between the UT and the satellite. Again, the distance is computed using the actual UT position and is given by

$$FSL = -20log\left(\frac{4\pi r}{\lambda_b}\right) \ (dB) \tag{6}$$

where $\lambda_b = f_b/c$ is the wavelength corresponding to frequency f_b of the beam and $c = 3 \times 10^8 m/sec$ is the speed of light.

B. Satellite EIRP in a beam

The signal from the satellite is a BCCH burst towards a beam and depends on the emitted power from the satellite antenna. For our purposes, the power P_{EIRP} increases linearly as a function of the beam distance from nadir to compensate for increased free space loss. For a specific beam, the received power near beam edge may be $3-5dB$ lower than that received at beam center, depending on the position of a beam in the footprint. For each beam, the power varies in a quadratic manner as a function of UT distance from the beam center. If the UT coordinates are translated in the OF coordinate system, then

$$P_{EIRP}(x) = P_{EIRP}(x_0) - \frac{\kappa\, x^2}{R_b^2}\ (dB) \tag{7}$$

for $x\epsilon\,[x_0, R_b]$, where $P_{EIRP}(x_0)$ is the EIRP value at beam center, R_b is the cell radius and $\kappa = P_{EIRP}(x = R_b) - P_{EIRP}(x = x_0)$.

C. Fading model

The fading model involves all multipath propagation mechanisms, including reflection, diffraction and scattering. Changes in path lengths in those propagation mechanisms occur according to the geometry of the surrounding environment and the received signal is a function of differences in the phase of the aggregate signal. Multipath fading is modeled by the Rayleigh or Rician model. The Rician fading model is similar to that for Rayleigh fading, except that a strong dominant (LOS) component is also present. The signal amplitude α follows the Rayleigh or Rice distribution with p.d.f respectively

$$f_\alpha(\alpha) = \frac{\alpha}{\sigma} \exp\left(-\frac{\alpha^2}{\sigma^2}\right) \tag{8}$$

$$f_\alpha(\alpha) = \frac{\alpha}{\sigma^2} \exp\left(-\frac{\alpha^2 + C_d^2}{2\sigma^2}\right) I_o\left(\frac{C_d \alpha}{\sigma^2}\right) \tag{9}$$

where σ^2 and $\frac{1}{2}C_d^2$ is the power of the scattered and the dominant signal and I_o is the modified Bessel function of first kind and zero order, defined as :

$$I_o(x) = \frac{1}{2\pi} \int_{-\pi}^{\pi} \exp\left(x \cos\theta\right) d\theta \tag{10}$$

The above mechanisms are simulated by the presence of S scatterers in the proximity of the UT actual position. Their positions are uniformly distributed in the area around the UT and the effect of distant multipath factors is considered negligible. In order to compute the fading loss, the length ℓ_i of the path followed by the signal affected by a particular scatterer i is computed and converted into a phase $\phi_i = 2\pi\ell_i/\lambda_b$. If we define the Rician factor K_R as the ratio of powers of the dominant and the scattered (multipath) signal

$$K_R = 10 \log \frac{C_d^2}{2\sigma^2}\ (dB) \tag{11}$$

the signal envelopes are found to be respectively

$$E_{Rayleigh} = \left[\left(\frac{1}{\sqrt{S}} \sum_{i=1}^{S} \sin\phi_i\right)^2 + \left(\frac{1}{\sqrt{S}} \sum_{i=1}^{S} \cos\phi_i\right)^2\right]^{1/2} \tag{12}$$

$$E_{Ri} = \frac{1}{1+V}\left[\left(\frac{1}{\sqrt{S}} \sum_{i=1}^{S} \sin\phi_i\right)^2 + \left(\frac{1}{\sqrt{S}} \sum_{i=1}^{S} \cos\phi_i + V\right)^2\right]^{1/2} \tag{13}$$

where for the Rician fading, a constant factor $V = 10^{K_R/20}$ was added in the in-phase component of the Rayleigh envelope.

D. Shadowing loss

The shadowing loss appears because of sudden obstructions of the path. Diversity operation is the primary means of mitigating heavy shadowing. Due to the extremely unpredictable nature of shadowing, it has not been included as part of the propagation model.

E. Received signal strength

The received aggreagate signal strength is:

$$P_{received} = P_{EIRP} + FSL + L_{atm} + G_{UT} + E_{fading} \tag{14}$$

where G_{UT} is the gain of the UT antenna and L_{atm} are additional atmospheric losses.

VI. Probability of beam handover

According to the combined handover algorithm, both the UT position and the received signal strength determine the handover decision. We derive an analytical expression of the probability of handover in this case.

Assume that $[0, R]$ represents the overlap area between two beams and that x is the mobile position, $x\epsilon\,[0, R]$. Let the signal strength received from each link be $A_i(x)$ under the influence of free space loss and fading effect, and $a_i(x)$ without fading effects for $i = 1, 2$. Then the difference of the two signals, $\Delta a(x) = |a_2(x) - a_1(x)|$ can be modeled as a Gaussian random variable, i.e $\Delta a(x) \sim N\left(\mu_\Delta(x), \sigma_\Delta^2\right)$ with

$$\mu_{\Delta(x)} = |A_2(x) - A_1(x)| \tag{15}$$

$$\sigma_\Delta^2 = 2\sigma^2 \tag{16}$$

where σ is the variance of the Rayleigh or Rice fading model. Let F be the threshold in signal strength difference. Then the probability of handover is

$$P_{h_1}(x) = Pr\left\{\Delta a(x) \geq F\right\} \tag{17}$$

Assume also that UT position inaccuracy U, follows a normal distribution, $U \sim N\left(0, \sigma_U^2\right)$. Then if the actual UT position is x and the estimated position is $\tilde{x}$ then $\tilde{X} \sim N\left(x, \sigma_U^2\right)$ and the probablity of handover, under UT position criterion is

$$P_{h_2}(x) = Pr\left\{\tilde{X} \geq x^*\right\} \tag{18}$$

where x^* is a nominal predetermined location threshold in the overlap area, where handover occurs. In the combined handover algorithm, a handover occurs if the signal strength and the UT position satisfy conditions 17 and 18 simultaneously.

VII. Simulation and results

A realistic satellite system environment has been built and a representative traffic distribution has been adopted. Specific terrestrial areas expose greater traffic density, whereas others (e.g. the poles, or areas covered by sea) are characterized by negligible traffic. Calls are assumed to arrive in independent Poisson streams while call hold times follow the exponential distribution with mean $150sec$. Depending on geographical location, the average satellite elevation angle varies between 30^o and 48^o and the azimuth separation angle varies between 65^o and 135^o. The contribution of those parameters and power measurements is taken into consideration, i.e $A = B = 1$ in equation 2.

In figure 4 satellite coverage as a function of latitude is depicted. Global coverage is verified. The possibility of two satellites being visible simultaneously is also high (more than 80%), providing the system with the capability to establish diversity. For low latitudes, even three satellites are visible sometimes $(40\% - 70\%)$ and for selected latitude regions $(10^o - 30^o)$ four satellites are also visible.

Regarding diversity path allocations, it was observed that a transition for one of the two paths occurs for at least 88% of the cases. The transition of both diversity paths depends on the the proximity of the diversity monitoring time point and the handover time instant and occurred for $2 - 12\%$ of the cases.

In figures 5 and 6 we present comparative results about satellite and beam handover rates under the UT Position and the Maximum Beam Residence criteria in a region with moderate load (0.92 calls per second). By using the latter criterion, a reduction to beam handover rate up to $85 - 90\%$ was observed in steady state, while for heavier traffic load this reduction reached $35\% - 40\%$. A small drawback is the increased satellite handover rate for some time periods. Taking into consideration the low satellite handover rate ($3-4$ handovers per minute in steady state), this fact should not receive further attention. At any rate, under heavy traffic, the satellite handover rate is reduced by more than 50% as well. The corresponding amount of signalling information associated with a handover event is accordingly reduced.

The worst case effect of UT mobility is considered by assuming that the UT moves in a direction opposite to that of the beam motion, with an average velocity of $72km/h = 0.02km/sec$. We consider the situation when a mobile experiences two successive handovers and moves in edge beams. The realistic assumption that the average time between beam handovers is $10min$ is adopted. From figure 7 it is evident that the worst case occurs when an edge beam moves at about $V_{e,min} = 0.75km/sec$. Then the actual transition time decreases by 2.5% for each transition, which, for the first $20min$ of a call is translated in a decrease of at most $44sec$. A very low percentage of calls is expected to be extended. In such cases, however, a safeguard mechanism would be to use measurements rather than UT position as a potential trigger for handover.

VIII. Conclusion

Two reliable criteria for handover prediction and resource allocation have been presented, the second of which minimizes signalling overhead. The effect of UT mobility and the application of a simplistic propagation model are also illustrated in the above context. Further study should focus on the enhancement of the above analyzed techniques in the context of channel allocation.

IX. Appendix A

Transformation matrix between ECEF and OF coordinate systems

The transformation matrix is a 3×3 matrix that relates the ECEF an d OF coordinate systems and is obtained as follows:

1. Get the satellite position and velocity vectors in the ECEF coordinate system, $\vec{P}(t)$ and $\vec{V}(t)$ and the corresponding magnitudes $|\vec{P}(t)| = R_E + h$ and $|\vec{V}(t)| = 2\pi(R_E + h)/T$.
2. Evaluate the vector $\vec{\gamma}(t) = -\vec{P}(t) \times \vec{V}(t)$.
3. Get the third row of the transformation matrix as:

$$\vec{r}_3 = -\frac{\vec{P}(t)}{|\vec{P}(t)|} \tag{19}$$

4. Get the second row of the transformation matrix as

$$\vec{r}_2 - \frac{\vec{\gamma}(t)}{|\vec{\gamma}(t)|} \tag{20}$$

5. Get the first row of the transformation matrix as

$$\vec{r}_1 = \vec{r}_2 \times \vec{r}_3 \tag{21}$$

X. Appendix B

Computation of elevation and azimuth separation angles

Let us denote by $\vec{S}(t)$ and $\vec{P}(t)$ the ECEF satellite and UT position vectors. A satellite is visible from the UT if its elevation angle relative to it,

$$\theta_{UT} = \cos^{-1}\left(\frac{-\vec{P}(t) \cdot \left[\vec{S}(t) - \vec{P}(t)\right]}{R_E \cdot |\vec{S}(t) - \vec{P}(t)|}\right) - \frac{\pi}{2} \tag{22}$$

is greater than 10^o. Similar visibility criteria hold for the SBS, the only difference being that the position vector of the SBS remains constant with time.

The azimuth separation angle is the angle on the earth surface between arc L_1 connecting UT position and subsatellite point S_1 of first satellite and arc L_2 connecting UT position and subsatellite point S_2 of second satellite.

The function $D(\cdot, \cdot)$ computes the distance of two points P_1, P_2 with given longitudes and latitudes $P_1(\phi_1, \theta_1)$ and

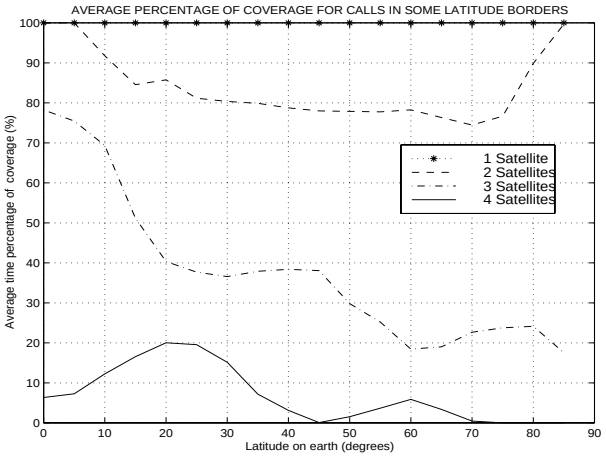

Fig. 4. Percentage of time coverage from one, two, three or four satellites, as a function of latitude.

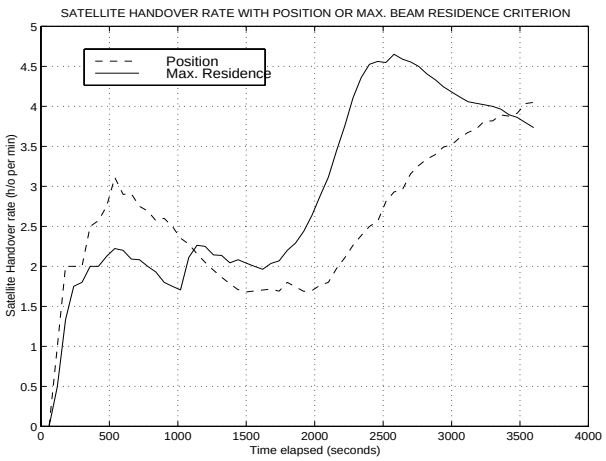

Fig. 5. Comparison of satellite handover rate under UT position or maximum beam residence time triggered handover event at a region with 0.92 calls/sec.

$P_2(\phi_2, \theta_2)$ on the earth as

$$D(P_1, P_2) = 2\tan^{-1}\left(\frac{\sin\alpha_x}{\sin\alpha_y}\tan\frac{a_1 - a_2}{2}\right) \tag{23}$$

where

$$\alpha_x = arctan\left(\frac{\cos((a_1 - a_2)/2)}{\cos((a_1 + a_2)/2)} \times \frac{1}{\tan(a_{12}/2)}\right) \tag{24}$$

$$\alpha_y = arctan\left(\frac{\sin((a_1 - a_2)/2)}{\sin((a_1 + a_2)/2)} \times \frac{1}{\tan(a_{12}/2)}\right) \tag{25}$$

and $a_1 = \pi/2 - \theta_1$, $a_2 = \pi/2 - \theta_2$,

$$a_{12} = \begin{cases} \phi_1 - \phi_2 & \text{if } \phi_1 - \phi_2 < \pi \\ 2\pi - (\phi_1 - \phi_2) & \text{otherwise} \end{cases} \tag{26}$$

The azimuth angle is calculated using spherical trigonometry

$$\phi_{azim} = \frac{\cos(D(S_1, S_2)) - \cos(D(S_1, UT))\cos(D(S_2, UT))}{\sin(D(S_1, UT))\sin(D(S_2, UT))} \tag{27}$$

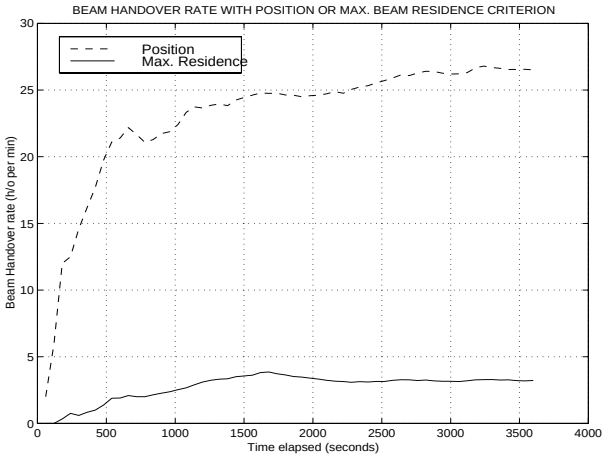

Fig. 6. Comparison of beam handover rate under UT position or maximum beam residence time triggered handover event at a region with 0.92 calls/sec.

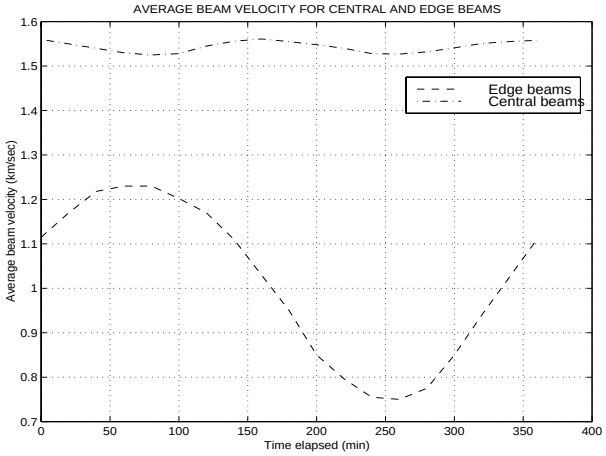

Fig. 7. Average beam velocity for central and edge beams as a function of time.

References

[1] D. Roddy : *Satellite Communications*, Mc Graw-Hill, 1996.
[2] T. E. Wisloff : *Dual Satellite path diversity and practical channel management for non-geostationary satellite systems*, 1996 5th IEEE International Conference on Universal Personal Communications.
[3] A. Böttcher and M. Werner : *"Strategies for Handover control in Low Earth Orbit Satellite systems"*, IEEE 44th Vehicular Technology Conference, 1994.
[4] F. Delli Priscoli : *"Functional areas of advanced mobile satellite systems"*, IEEE 47th Vehicular Technology Conference, 1997.
[5] F. Ananasso and F. Delli Priscoli : *"Technology and Networking issues in 3^{rd} generation satellite personal communication networks"*, Third Annual ICUPC, 1994.
[6] F. Vatalaro, G. E. Corazza, C. Caini and C. Ferrarelli : *"Analysis of LEO, MEO and GEO Global Mobile Satellite Systems in the presence of interference and fading"*, IEEE Journal on Selected Areas in Communications, vol. 13, no. 2, February 1995.